Specificity of Lipid Incorporation Is Determined by Sequences in the N-Terminal 37% of ApoB†

Margaretha Carraway,*,‡,§ Haya Herscovitz,‡ Vassilis Zannis,§ and Donald M. Small‡

Department of Biophysics and Department of Medicine, Cardiovascular Institute, Center for Advanced Biomedical Research at Boston University School of Medicine, 715 Albany Street Boston, Massachusetts 02118-2526

Received April 7, 2000; Revised Manuscript Received June 15, 2000

ABSTRACT: The N-terminal 17% of apolipoprotein B (apoB-17) is secreted lipid-poor while apoB-41 particles are secreted with a triacylglycerol (TAG)-rich core. Thus, the sequence between apoB-17 and apoB-41 is necessary for the assembly of TAG-rich lipoproteins. To delineate this region, C127 cells were permanently transfected to secrete the N-terminal 29, 32.5, or 37% of apoB. Density gradient centrifugation showed that secreted apoB-29, apoB-32.5, and apoB-37 had peak densities of 1.25, 1.22, and 1.16 g/mL and percent lipid of particle weights of 30, 37, and 49%, respectively. Calculated anhydrous particle diameters were: apoB-29 = 81 Å, apoB-32.5 = 88 Å, and apoB-37 = 101 Å. Immunoprecipitated particles labeled with [^{3}H]oleate showed that, as apoB length increased from apoB-29 to apoB-32.5 and apoB-37, the number of TAG (core) molecules per apoB particle increased almost 16-fold from 8 to 32 to 124, while phospholipids and diacylglycerols (surface lipids) increased only slightly from 71 to 87 to 97 molecules, respectively. Thus, sequences in the C-terminus of apoB-29 bind phospholipids and diacylglycerols, sequences between apoB-29 and apoB-32.5 augment TAG binding and sequences between apoB-32.5 and apoB-41 account for the marked incorporation of TAG at a rate of ∼1 TAG per 2 amino acids. Cryoelectron micrographs of isolated apoB-37 particles revealed mostly spherical particles of ∼110 Å (11.0 nm) with an electron lucent center, consistent with these particles having a TAG core. We suggest that the predicted amphipathic β-sheets beginning at apoB-29, starts to preferentially recruit core lipids into apoB and propose that the consistent presence of DAG in the secreted particles may have a role in fission of the nascent lipoprotein particles from the endoplasmic reticulum membrane.

Apolipoprotein B (apoB)[1] is the major protein in low density lipoproteins (LDL) and serves as the ligand for the LDL receptor (*1*). It is the LDL receptor/apoB interaction that clears LDL from the plasma and thereby regulates cholesterol biosynthesis (*1*). In the plasma of healthy humans two natural forms of apoB are present: apoB-100 and apoB-48. ApoB-100 is synthesized in the liver and secreted on very low-density lipoproteins (VLDL). ApoB-48 is formed in the intestine by posttranscriptional modification of apoB-100 mRNA and corresponds to the N-terminal 48% of apoB-100 (*2*). ApoB-48 encodes all the structural elements required for the formation and secretion of chylomicrons and VLDL (*3*).

Mutations in the apoB gene in humans have been identified that cause truncations ranging from apoB-2 to apoB-89. Truncations in apoB, as well as other genetic disorders, can lead to familial hypobetalipoproteinemia (HBLP) (*4*−*7*). HBLP is an autosomal co-dominant trait associated with low plasma levels of cholesterol and apoB-containing lipoproteins such as LDL. Heterozygous HBLP patients can be asymptomatic, but homozygous individuals may show severe neuropathies due to mal-absorption of intestinal fat and fat-soluble vitamins (*4, 5*). Both in vivo and in vitro experiments indicate that low plasma levels of truncated apoB forms can result from changes in the rate of synthesis, efficiency of translocation, degree of degradation or enhanced clearance of apoB-containing lipoproteins from plasma (*8*−*11*).

An inverse correlation between the length of apoB and the density of secreted apoB-containing lipoproteins has been observed in the plasma of patients with HBLP (*4, 5*). The decrease in particle density, due to increased association with lipids of the longer truncated apoB forms, has also been observed in in vitro studies in human (HepG2) (*12*−*16*) and rat hepatoma-derived cells (*13, 17*−*20*) transfected with human cDNAs encoding various lengths of apoB (*21*).

We have previously shown that mouse mammary carcinoma-derived (C127) cells, transfected to express the N-terminal 17% of human apoB (apoB-17), secreted predominantly lipid-poor apoB-17 with a peak density >1.21 g/mL (*22*). In contrast, apoB-41 was secreted on HDL-sized particles with a peak density of 1.13 g/mL. Lipid analysis of the secreted particles revealed a TAG-rich core (*23*). These data indicate that the sequence between the N-terminal 17% and 41% is critical for the assembly and subsequent secretion of apoB-containing lipoproteins with a TAG-rich core.

† This work was supported by NIH Grant HL-26335 and BUMC cardiovascular Institute Grant HL-07224-23.

* To whom correspondence should be adressed. Phone: (617) 638-4084. Fax: (617) 638-4041. E-mail: carrraway@med-biophd.bu.edu.

‡ Department of Biophysics.

§ Department of Medicine.

[1] Abbreviations: apoB, apolipoprotein B; TAG, triacylglycerols; PL, phospholipids; DAG, diacylglycerols; CE, cholesterol esters; HDL, high density lipoproteins; LDL, low density lipoproteins; ER, endoplasmic reticulum.

10.1021/bi000791h CCC: $19.00
Published on Web 07/20/2000

To refine the minimum N-terminal region of apoB needed for the assembly and secretion of TAG-rich apoB-containing lipoproteins, stable transfected C127 cell lines were generated to express truncated forms of apoB corresponding to the N-terminal 29, 32.5, and 37% designated, apoB-29, apoB-32.5, and apoB-37, respectively. Density gradient centrifugation and immunoprecipitation with antibodies to apoB showed that a fraction of secreted apoB-29 was found at density ≥1.31 g/mL. In contrast, none of the secreted apoB-32.5 or apoB-37 were found at density >1.29 g/mL indicating that these apoB forms are secreted exclusively associated with lipids. Lipid analysis demonstrated that surface lipids were the major lipids associated with secreted apoB-29. The data further demonstrated that as the length of apoB increases so does core lipid incorporation. Thus, while apoB-29 has only 11% of its lipids as core lipids, apoB-32.5 has 28% and apoB-37 has 58%. Therefore, core lipids are the major lipids associated with secreted apoB-37. We conclude that the β-sheets at and beyond apoB-29 are critical for recruiting TAG into nascent lipoproteins.

MATERIALS AND METHODS

Materials. Materials were purchased from the following sources: restriction and modifying enzymes from New England Biolabs. Dulbecco's modified Eagle's medium (DMEM), methionine- and cysteine-free DMEM, Dulbecco's phosphate buffered saline, pH 7.4 (DPBS), and fetal calf serum from Life Technologies, Inc. [^{35}S]Methionine/cysteine Expre^{35}S^{35}Sprotein labeling mix (specific activity > 1000 Ci/mmol), [^{3}H]oleate (specific activity 2−10 Ci/mmol), and reagents for enhanced chemiluminescent detection system (ECL) from NEN life Science products. *N*-Acetyl-leucinyl-leucinyl-norleucinal (ALLN) was purchased from Boehringer Mannheim, 4-[2-aminoethyl] benzylsulfonylfluoride (AEBSF) from Calbiochem and leupeptin and aprotonin from Sigma. Goat polyclonal antibodies to human apoB were from BioDesign. Centricon Centrifugal Filter Devices YM-30 were from Amicon.

Expression Plasmids and Intermediate Constructs Containing apoB cDNA Sequence. A construct containing the apoB-46 sequence in a pUC plasmid derivative was generated by ligating the fragments *Pvu*II to *Bcl*I (nt 121 to nt 832) and *Bcl*I to *Eco*RI (nt 832 to nt 6497) of apoB cDNA into sites of plasmid pUC48 via a triple ligation reaction. The plasmid pUC48 was constructed by replacing the polylinker region of pUC18 with a synthetic region containing the restriction sites *Bss*HII-*Xho*I-*Pvu*II-*Bam*HI-*Cla*I-*Eco*RI-*Sal*I-*Mlu*I-*Not*I-*Xho*I. The resulting plasmid designated pUB-47 was digested with *Bss*HII and *Xho*I and cloned into the corresponding sites of papilloma virus-based expression vector (pBMT3XM) to generate plasmid pBMB-29. pBMT3XM was derived by modification of the original pBMT3X vector which contains the restriction sites *Xho*I, *Bss*HII, and *Not*I, and is under the control of mouse metallothioneine-1A (*23*).

To generate the expression plasmids containing the apoB-32.5 sequence, pUB-47 was digested with *Bss*HII and *Bam*HI to release a *Bss*HII−*Bam*HI fragment (nt 121 to nt 2542) and a *Bam*HI−*Bam*HI fragment (nt 2542 to nt 4908). These fragments were cloned into the modified pGEM7Z-4 vector in two steps. The polylinker of this vector has been modified to include the *Aat*II, *Bss*HII, *Bam*HI, *Not*I, and *Sal*I sites. The *Bss*HII, the *Bam*HI fragment was cloned first in this vector, followed by the *Bam*HI−*Bam*HI fragment. The orientation of the *Bam*HI−*Bam*HI fragment was confirmed with *Xho*I restriction analysis and designated plasmid pGAB-16. The apoB-32.5 cDNA insert was excised from pGAB-16 and cloned into the corresponding sites of the pBMT3XM vector to generate pGB32−16. The expression plasmid containing the apoB-37 sequence was made by digesting pUB-47 with *Bss*HII and *Sal*I (nt 121 to 5280) and this cDNA fragment was cloned into the corresponding sites of the pBK−CMV vector to generate pGAB-13. The apoB-37 cDNA was excised with *Bss*HII and *Not*I from pGAB-13 and cloned into corresponding sites of pBMT3XM to generate plasmid pGB37−20. The correct reading frame of apoB-29, apoB-32.5, and apoB-37 into pBMT3XM vector was verified by DNA sequencing.

Cell Culture and Metabolic Labeling. C127 cell lines, expressing truncated forms of apoB, were grown as described previously (*23*). Exponentially growing cells were plated in a 100 mm-diameter dishes and incubated in DMEM containing 10% fetal calf serum (growth media). Experiments were initiated when cells were 70−80% confluent. Cells were incubated overnight in three different media: growth media alone, growth media supplemented with 0.2 mM albumin, or 0.8 mM oleate complexed to 0.2 mM albumin (4:1 molar ratio, respectively). Cells were then washed with DPBS and preincubated in methionine- and cysteine-free DMEM (labeling media) for 2 h. Cells were washed again with DPBS and labeled with [^{35}S]methionine/cysteine and [^{3}H]oleate complexed to albumin (4:1 molar ratio) for 6 h in labeling media suplemented with albumin or oleate as above. Media were then adjusted to 200 μM methionine/300 μM cysteine to enhance protein synthesis, and incubation proceeded overnight.

Density Gradient Centrifugation. After overnight incubation conditioned media were collected and adjusted to 5 mM EDTA and 0.02% NaN_3. The protease inhibitors ALLN, leupeptin, and aprotonin were added to a final concentration of 10 μg/mL each and AEBSF to 0.1 mM. The culture media were centrifuged at 800*g* for 5 min in J-6 centrifuge (Beckman) to remove cell debris. The supernatants were adjusted with solid CsCl or KBr as described below and subjected to density gradient centrifugation in SW41 Ti rotor at 10 °C. ApoB-29 and apoB-32.5 containing media were adjusted with solid CsCl to 1.4 g/mL, overlayered with a CsCl solution of 1.20 g/mL and centrifuged at 31K rpm for 66 h. ApoB-37-containing media was adjusted to 1.25 g/mL with KBr, overlayered with a KBr solution of 1.08 g/mL and spun at 40 k rpm for 72 h. Twelve fractions of 1.0 mL each were collected from the top of the centrifuge tubes and their densities calculated from refractive index measurements with Abbe Refractometer model 10450 (American Optical Corporation, Buffalo, NY). Density fractions were dialyzed into PBS/0.05% azide using micro concentrators equipped with 30K MW cutoff membranes. The cells were washed with ice-cold DPBS and solubilized by incubation in 1% Triton X-100-PBS, pH 7.4, for 30 min in the presence of the above-mentioned protease inhibitors. Cell lysates were centrifuged at 13000*g* in a microcentrifuge for 15 min at 4 °C to remove cell debris. Postnuclear fractions were subjected

to immunoprecipitation alongside density fractions as described below.

Immunoprecipitation, SDS−PAGE, and Immunoblotting. Cell lysates or density fractions were precleared with gelatin- and protein G-Sepharose and incubated overnight at 4 °C with goat antiserum to human apoB, and immunocomplexes were captured on protein G-Sepharose beads by incubation for 45 min. The beads that were incubated with cell lysates were first washed with 1% Triton X-100/PBS, then with 0.5% SDS/0.5% Triton X-100/PBS and finally with PBS. The beads that were incubated with the density fractions were washed with PBS alone. The protein was extracted from the beads by boiling in sample buffer (*24*) containing 10% β-mercaptoethanol and 6M urea for 3−5 min and analyzed by 6−10% SDS−polyacrylamide gel electrophoresis followed by autoradiography using a PhosphorImager (Molecular Dynamics)

Lipid Analysis. ^{3}H-Labeled lipids associated with secreted apoB forms were dissociated from the protein G-Sepharose beads by two extractions with 1 mL of chloroform/methanol (2:1, vol/vol), supplemented with appropriate standards, separated by thin-layer chromatography, identified by iodine vapors, scraped, and quantified by liquid scintillation spectrometry (*23*). The amount of lipid associated with the secreted particles was initially calculated from the relative composition of lipids and converted to number of molecules for individual lipid as follows. Weight % of lipid = volume % lipid × FW of lipid. Factor 1 = MW of protein/FW of protein. Number of lipid molecules = factor 1 × weight % of lipid/MW of lipid. Calculations were made using MW: PL = 787, DAG = 621, CE = 650, TAG and "X" = 850.

Calculations of Protein and Lipid Mass, and Particle Volume and Size as an Anhydrous Sphere. Calculations were made assuming molecular weights (MW) of 513000 for nonglycosylated apoB and densities of 0.9 g/mL for TAG, "X", and CE; 0.91 g/mL for DAG; 1.0 g/mL for PL and 1.369 g/mL for protein. The MW of truncated proteins was calculated based on the number of amino acids using Protein Sequence Shareware Version 1.2. Lipid densities were based on percent total lipids measured in secreted particles as described above. The following equations were used for the remaining calculations. Formula weight (FW) of protein = (particle density − lipid density)/(protein density − lipid density). FW of lipid = 1 − FW of protein. MW of lipid = (FW of lipid × MW of protein)/FW of protein. Volume (V) of protein (Å^3) = (MW of protein/density) × (10^{24} Å^3/Avogadro's number). V of lipid (Å^3) = (MW of lipid/density) × (10^{24} Å^3/Avogadro's number). V of particle (Å^3) = V of protein + V of lipid. Radius of particle calculated as a sphere = $\sqrt[3]{V/(4/3\pi)}$.

Electron Microscopy. (i) Negative Staining. ApoB-37 containing particles were prepared and negatively stained as described (*22*, *23*) with the following modification. A 3 μL aliquot was taken from just below the meniscus at the top edge of the density gradient tube (density 1.195) and added to 6 μL of pure water on a grid. After 30 min incubation, the grid was rinsed with pure water, stained with 1% sodium phosphotungstate, pH 7.4, and air-dried.

(ii) Cryoelectron Microscopy. As described above, a 3 μL aliquot containing the lipoprotein particles was placed on a holey coated carbon film covering a 400 mesh copper grid and plunged into liquid ethane at liquid N_2 temperature of 77 K to trap the particles in vitreous ice. Cryotransmission electron microscopy was carried out as described previously (*25*, *26*). Images were recorded under low dose conditions at a defocus of 1.5 μm in a Philips CM-12 transmission electron microscope. Particle measurements were made directly from negatives.

RESULTS

Density Distribution of apoB-Containing Particles. C127 cell lines expressing either apoB-29, apoB-32.5, or apoB-37 protein were generated and characterized. The cell lines secreting the highest levels of apoB forms were used for further studies. Secreted apoB forms were analyzed following incubation of cells in media (data not shown) or media supplemented with either 0.2 mM albumin or 0.8 mM oleate complexed to 0.2 mM albumin (Figure 1, A and B). Density gradient centrifugation of the secreted proteins, followed by immunoprecipitation with antibodies to apoB and autoradiography, showed peak densities of 1.25, 1.22, and 1.16 g/mL for apoB-29, apoB-32.5, and apoB-37, respectively (Figure 1). The three cell lines secreted more particles with lower densities when incubated with oleate. Despite this observed shift, the peak densities of the secreted particles did not change (Figure 1). While 17% of apoB-29 was recovered at a density of ≥1.31 g/mL, no apoB-37, or apoB-32.5 protein were detected at a density of >1.29 g/mL (Figure 1). Incubated in the presence of oleate, C127 cells expressing apoB-32.5 generated an additional smaller peak at a density of ≤1.18 g/mL in CsCl (Figure 1) and KBr gradients (data not shown). This peak represents 14% of the total secreted apoB-32.5. Thus, in the presence of oleate, apoB-32.5 is secreted on two distinct populations of lipoproteins.

Further, the amount of secreted apoB-37 increased 8-fold, upon incubation of cells with 0.8 mM oleate, compared to the corresponding controls. In contrast, the amount of secreted apoB-32.5 and apoB-29 did not change in the presence of 0.8 mM oleate (Figure 1).

Analysis of Labeled Lipids Associated with Secreted apoB Forms. Analysis of [^{3}H]oleate-labeled lipids showed (Table 1) that following incubation of cells with 0.8 mM oleate, secreted apoB-29 was associated with 69% phospholipids (PL), 20% diacylglycerols (DAG), 6% TAG, 3% of a previously described core lipid "X" (*23*), and 2% cholesterol esters (CE). Analysis of "X" shows it to be a mono-alkyl DAG (*23*). Table 1 shows that secreted apoB-32.5 was associated with 59% PL, 13% DAG, 17% TAG, 6% "X", and 5% CE. ApoB-37 was secreted with 39% PL, 3% DAG, 50% TAG, 4% "X", and 4% CE. Thus, the shorter apoB-29 form is secreted with a total of 89% surface and 11% core lipids, the intermediate apoB-32.5 with 72% surface and 28% core lipids and the longer apoB-37 with 42% surface and 58% core lipids (Table 1). We have previously reported (*23*) that apoB-41 was secreted associated with 32% surface and 68% core lipids (Table 1). These data show that as apoB increases in size, percent of surface lipids decreases concurrently with an increase in percent core lipids (Table 1). The number of core lipid molecules (TAG, "X", and CE) associated with apoB-29, apoB-32.5, apoB-37, and apoB-41 containing particles corresponds to 8, 32, 124, and 199,

Table 1: Composition of [^{3}H]Oleate-Labeled Lipids Associated with apoB-29, apoB-32.5, apoB-37, and apoB-41 Secreted by C127 Cells[a]

	apoB-29	apoB-32.5	apoB-37	apoB-41[b]
Percent of Total Lipids				
PL	69	59	39	26
DAG	20	13	3	6
TAG	6	17	50	62
"X"	3	6	4	4
CE	2	5	4	2
surface lipids (PL, DAG)	89	72	42	32
core lipids (TAG, "X", CE)	11	28	58	68
Calcd No. of Lipid Molecules per Particle				
PL	52	68	88	81
DAG	19	19	9	24
TAG and "X"	6	25	113	191
CE	2	7	11	8
surface lipids (PL, DAG)	71	87	97	105
core lipids (TAG, "X", CE)	8	32	124	199
total lipid molecules	79	119	221	304

[a] Cells were incubated, and lipids extracted and analyzed as described in Figure 2. [b] Ref *23*.

respectively (Table 1, Figure 2), an increase of over 24-fold between apoB-29 and apoB-41. In contrast, the number of surface lipid molecules (DAG and PL) associated with apoB-29, apoB-32.5, apoB-37, and apoB-41 changes moderately: DAG correspond to 19, 19, 9, and 24 molecules and PL to 52, 68, 88, and 81 molecules, a 1.3- and 1.5-fold increase, respectively (Table 1, Figure 2).

Electron Microscopy. Negative-stain EM showed a generally rounded shape apoB-37-containing lipoprotein particles. A total of 508 secreted particles were measured, and 90% ranged in size between 6.7 and 22.2 nm, 5% were <6.7 nm and 5% were greater than 22.2 nm (Figure 3A). The average size of all particles observed under negative stain was 11.7 nm (Figure 3A). The major peak occurs at ~11 nm but a second peak appears at ~22 nm consistent with a small population of LDL-sized particles.

Cryotransmission electron microscopy of apoB-37 particles prepared in vitreous ice (Figure 3B) revealed that 94% of 219 measured particles were between 6.7 and 22.2 nm, 5.5% were <6.7 nm and 0.5% >22.2 nm (Figure 3C). The average size of particles observed with cryotransmission electron microscopy was 11.0 ± 4.2 nm (Figure 3B). However, the distribution has an extension to around 22.2 nm suggesting a small population of larger apoB-37 particles similar to those seen in negative stain (Figure 3A). The particles show quasi-spherical shape with electron density concentrated largely at the surface (Figure 3B) consistent with a microemulsion particle with a less electron dense TAG in the core, and PL and protein on the surface. Some particles show a dense protrusion that is consistent with the N-terminal 6−10% of apoB forming a separate surface domain (*27*−*29*).

Calculations of the Size of Secreted apoB Containing Particles. The truncated forms of apoB used in this study, apoB-29, apoB-32.5, and apoB-37 are composed of 1306, 1481, and 1695 amino acids, respectively (Table 2). The calculated molecular weight for nonglycosylated apoB-29, apoB-32.5, and apoB-37 is 146 232, 165 783, and 188 996, respectively. Combining these figures with the measured peak densities and lipid composition of the apoB-containing particles (Table 2) described in this study, we calculated the following parameters (Materials and Methods). The lipid densities of apoB-29, apoB-32.5, and apoB-37 are 0.97, 0.96, and 0.94 g/mL, respectively. The respective fractional weights of total lipids are 0.30, 0.37, and 0.49 with a lipid molecular weight of 62 371, 95 116, and 178 977 (Table 2). The fractional weight of total protein weights is 0.70, 0.63, and 0.51 for apoB-29, apoB-32.5, and apoB-37, respectively. The calculated anhydrous volumes are 283 996, 365 509, and 545 570 Å^3. Assuming a spherical particle the diameters are 8.1, 8.8, and 10.1 nm for apoB-29, apoB-32.5, and apoB-37, respectively (Table 2). A comparison (Figure 4) between volume of secreted particles with number of amino acids present in the truncated forms of apoB reveals a linear relationship (R-value: 0.979; p-value of 0.02).

DISCUSSION

In this study, we demonstrate by lipid analysis that apoB-37 is secreted associated with almost three times more lipid molecules than apoB-29 (Table 2, Figure 2). This disproportionate increase in lipid content relative to apoB length explains the observed decrease in densities associated with longer apoB proteins. The peak densities, of the secreted apoB-29, -32.5, and -37 particles were 1.25, 1.22, and 1.16 g/mL. These peak densities observed in C127 cells agree extremely well with peak densities of truncated apoB-32.5 and apoB-37 observed in human studies reported at >1.21 and 1.12-1.15 g/mL, respectively (*30*, *31*). Because until now, no detectable levels of apoB-29 have been observed in human plasma, no comparison can be made for the apoB-29 in C127 cells (*5*).

The decrease in particle density with increasing length of apoB protein has been reported both in vivo (*4*, *5*) and in vitro, i.e., HepG2 (*13*, *14*, *16*, *32*), as well as McArdle RH-7777 cells (*13*, *17*−*20*). Although in these systems variations in densities for a specific truncated apoB form have been reported, the same inverse relationship within each expression system is maintained (*21*). The involvement of molecular chaperones in the assembly and secretion of both full length and truncated apoB forms has been documented (*33*−*39*). We suggest that the observed variations in densities of a given truncated apoB protein in the individual cell system reflect differences in the profile of chaperones that interact with apoB to mediate its maturation.

This study also demonstrates that cells, grown in the presence of 0.8 mM oleate, secreted lipoprotein particles with slightly lower densities in all three truncated apoB forms (Figure 1) although the density of the major peak does not change. We believe that the increased lipid availability resulted in extra lipid recruitment by all three truncated proteins and the formation of additional particles with lower densities (Figure 1A). Addition of oleate during cell growth did not increase the amount of secreted apoB-29 or apoB-32.5 protein. In contrast, apoB-37 was secreted 8-fold more efficiently in the presence of 0.8 mM oleate (Figure 1A). Thus, apoB-37 in C127 cells, grown in the presence of 0.8 mM oleate, responds more like apoB-100 in HepG2 cells (*40*) and apoB-41 in C127 cells (*23*). This fact argues that TAG availability to truncated forms such as apoB-37 facilitates their secretion and inhibits their degradation. On the other hand, it appears that lipidation with surface lipids in the shorter forms such as apoB-29 neither drives secretion or prevents degradation.

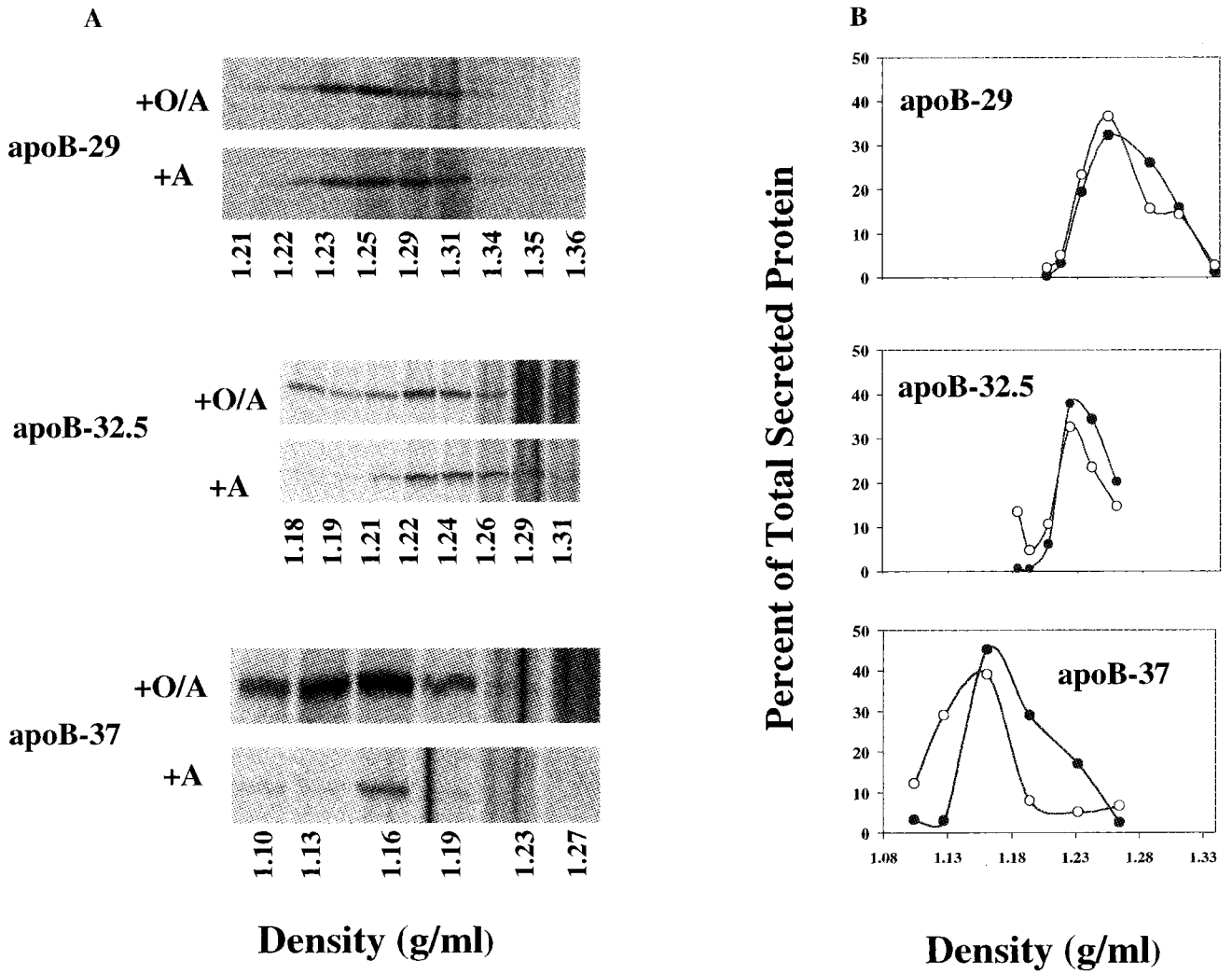

FIGURE 1: Density distribution of secreted apoB-29, apoB-32.5, and apoB-37. Cells were labeled with [^{35}S]methionine/cysteine in the presence of 0.2 mM albumin (+A) or 0.8 mM oleate/0.2 mM albumin (+OA) overnight as described in Materials and Methods. The culture medium was collected and subjected to density gradient ultracentrifugation as described in Materials and Methods. Density fractions were immunoprecipitated and analyzed by SDS−PAGE and autoradiography (A) as described in Materials and Methods. ApoB-29 and apoB32.5 were separated by CsCl, and apoB-37 by KBr density gradient. The intensities of apoB bands in panel A were quantified with ImageQuant program as described in Materials and Methods (B). Open circles represent cells incubated with 0.8 mM oleate/0.2 mM albumin, closed circles represent cells incubated with 0.2 mM albumin.

The average particle size of apoB-37 measured with negative staining and cryotransmission electron microscopy was 11.7 and 11.0 nm, respectively, and agrees very well with our calculated anhydrous diameter of 10.1 nm based on density, lipid and protein composition (Table 2). In addition, 90 and 94% of apoB-37 particles measured with negative staining and cryotransmission electron microscopy, respectively, ranged between 6.7 and 22.2 nm (Figure 3, panels A and C) and is consistent with particle size reported for apoB-32 in human plasma (*41*).

Not only do we observe additional lipid recruitment as apoB becomes longer, we also show that the volume percent of core lipids associated with apoB-37 increases 5-fold compared to those associated with apoB-29 (Table 1, Figure 2). This shift in lipid composition is not due to a decreased incorporation of surface lipids but is rather due to a greater than 10-fold increase of the core lipid TAG in the longer apoB-37 (Table 1, Figure 2). As a result, the smaller apoB-29 is secreted primarily with surface lipids while the larger apoB-37 is secreted with mostly core lipids. Together these data suggest that the β-sheets beyond apoB-29 not only incorporates more lipids but also preferentially recruits the core lipid TAG.

Computer modeling along the amino acid sequence of apoB-100 identified five regions: (1) an α/β mixed region between the N-terminal of apoB and apoB-20; (2) a β-sheet rich region between apoB-20 and apoB-43; (3) an α-helical rich region (apoB-42 to apoB-55); (4) a second β-rich region (apoB-55 to apoB-90); and (5) an α-rich C-terminal region (*42*−*44*). The N-terminal domain up to apoB-20 contains α-helices and amphipathic β-sheets. This N-terminal region was demonstrated to be essential for secretion of apoB (*14*, *45*−*49*) and has high homology to microsomal triglyceride transfer protein (MTP) and lipovitellins (*28*, *50*). The X-ray crystal structure of lamprey lipovitellin (*29*) shows that this homologous region could form part of a "lipid pocket" domain (*28*, *50*). Small and Atkinson (*44*) predicted that the region between apoB-21 and apoB-41 contained at least 41 amphipathic β-strands (ABS) 11 amino acids long or longer. ABS have a strong lipid binding capacity and their direct binding to TAG is energetically favored (*44*). Indeed, this β-sheet region of apoB is shown to be involved in lipid

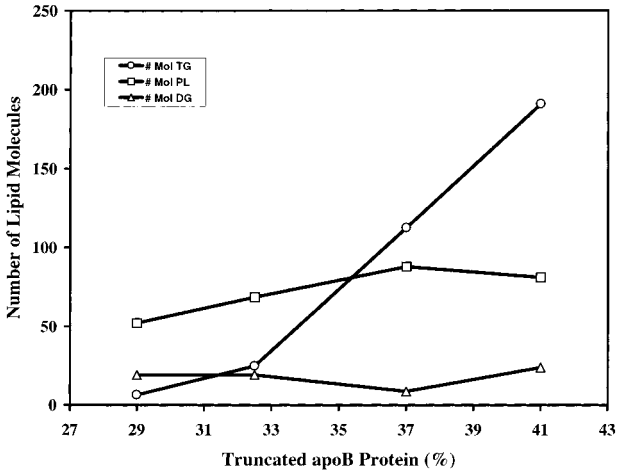

FIGURE 2: Number of lipid molecules associated with secreted apoB-29, apoB32.5, apoB-37, and apoB-41 lipoproteins. Cells were labeled with [^{3}H]oleate in the presence of 0.8 mM oleate/0.2 mM albumin overnight as described in Materials and Methods. Lipids were extracted from all density fractions and analyzed by thin-layer chromatography and quantified by liquid scintillation spectrometry as described in Materials and Methods. Data for apoB-41 are taken from ref *23*. Note that there is a modest increase in phospholipids between apoB-29 and apoB-37. DAG are found in small amounts in all particles. TAG increase slightly between apoB-29 and apoB-32.5, but then increase greatly at ratio of 1 TAG molecule per 2.3 amino acid residues between apoB-32.5 and apoB-41.

Table 2: Composition of Secreted apoB-29, apoB-32.5, and apoB-37 Lipoprotein Particles[a]

	apoB-29	apoB-32.5	apoB-37
total no. of amino acids	1306	1481	1695
MW protein	146 232	165 783	188 996
particle peak density (g/mL)	1.25	1.22	1.16
lipid density (g/mL)	0.97	0.96	0.94
fractional weight total lipid	0.30	0.37	0.49
MW lipid	62 371	95 116	178 977
fractional weight total protein	0.70	0.63	0.51
volume protein (Å^3)	177 348	201 059	229 211
volume lipid (Å^3)	101 648	164 450	316 358
volume of particle (Å^3)	283 996	365 509	545 570
radius Å (anhydrous spherical particle)	40.6	44.2	50.5
diameter (nm)	8.1	8.8	10.1

[a] The composition was based on numbers described in Figure 4 and calculated as described in Materials and Methods. Calculations use nonglycosylated apoB-100 MW 513.000, TAG (CE + "X") = 0.90; PL = 1.0; DAG = 0.9.

binding to form VLDL-like particles (*17*, *20*) in hybrid apoB constructs (*15*) as well as in chimeras between apoA1 and apoB (*17*).

The assembly of TAG-rich lipoproteins has been proposed to occur through two major steps (*32*, *51*−*54*). The first step involves the co-translational formation of a primordial particle of HDL and LDL density as apoB is translocated across the rough endoplasmic reticulum (ER) membrane. In a second step, this small particle can be enlarged, either gradually and/or through fusion with a TAG-rich particle to form nascent chylomicrons or VLDL (*51*−*54*).

The formation of the small PL-rich TAG-poor particle by apoB-29 observed in C127 cells (Table 1) is consistent with the hypothesis that the initial steps in lipoprotein assembly primarily involve the recruitment of phospholipids by the N-terminal region of apoB (*53*). This region encompasses the first 1000 amino acids and is proposed to form part of a "lipid pocket" (*28*, *50*). As apoB length increases beyond apoB-29, a lighter lipoprotein particle is formed due to recruitment of core lipids. This preferential core lipid incorporation continues when apoB is extended beyond apoB-32.5 to apoB-41 (Figure 2). This increased lipid incorporation is reflected by volume comparison between protein and lipids associated with truncated apoB forms. The lipid:protein volume ratios increases from 1:1.7 in apoB-29, to 1:1.2 in apoB-32.5, and to 1:0.7 in apoB-37 and is consistent with an increased capacity of apoB-37 to recruit more TAG to form the "primordial" particle as part of the first step of VLDL assembly (*51*−*54*).

Using a multi-algorithmic approach to predict amphipathic secondary structure, (*42*, *55*, *56*), we found that greater than 60% of the amino acids in the domain apoB-21 to apoB-41 were in amphipathic β-sheets (*44*). Two significant amphipathic helical regions were identified, one at apoB-21 and the second cluster of three amphipathic alpha helices centered at apoB-26.7. To specifically define the amphipathic β-sheet regions, we used a minimum window of $\pm$5 amino acids and slid this window along the sequence to identify amphipathic β-strands of 11 residues or longer. The cut off at 11 amino acids was used because it represents a strand of adequate length to span across a membrane and also to fit within the estimated width of apo-B of 40−60 Å on LDL (*3*). The criteria to identify the amphipathic β-strands were as follows: (1) it must have a strongly hydrophobic face, (2) no charged groups were allowed in the hydrophobic face and only one strongly polar amino acid (N, Q, or H) was allowed in the hydrophobic face, and (3) only one hydrophobic amino acid was allowed in the hydrophilic face. Using these criteria 41 amphipathic β-strands of 11−15 residues were identified between amino acids 968 and 1882 (apoB-21 to apoB-41). There were 11 between apoB-21 and apoB-29, 6 between apoB-29 and apoB-32.5, 11 between apoB-32.5 and apoB-37, and from apoB37 to apoB-41 there are 10 amphipathic β-strands.

Our data suggest a model for the formation of the "primordial" lipoprotein particle by a multistep process involving the initial recruitment of PL by the N-terminal region followed by incorporation of core lipids directed by the presence of β-sheets at and beyond apoB-29 (Figure 5). We propose that the N-terminal 20% of apoB, which has strong homology to lipovitellin (*29*, *50*), interacts with the internal phospholipid leaflet of the endoplasmic reticulum (ER) by amphipathic structures, mainly β-sheets, present between apoB-13 and apoB-20 (Figure 5A). This region is homologous to the lipovitellin C sheet and the first half of the A sheet (*28*, *29*). In cells having MTP, the B sheet region (residues 722−802) of MTP are suggested to close the cavity and allow the apoB/MTP complex to bind phospholipid as a bi-layer (*50*). However, in the absence of MTP, another part of apoB may close the cavity. We propose that the amphipathic β-sheets between apoB-21 and apoB-29 and the two α-helical regions at apoB-21 and apoB-26.7 serve this purpose and permit the formation of the PL-rich apoB-29 particle. We suggest that the recruitment of TAG is due to its association with the long, almost uninterrupted, region of the 28 predicted amphipathic β-strands (*44*) extending from apoB-29 to apoB-41 (Figure 5A). Of the 575 amino

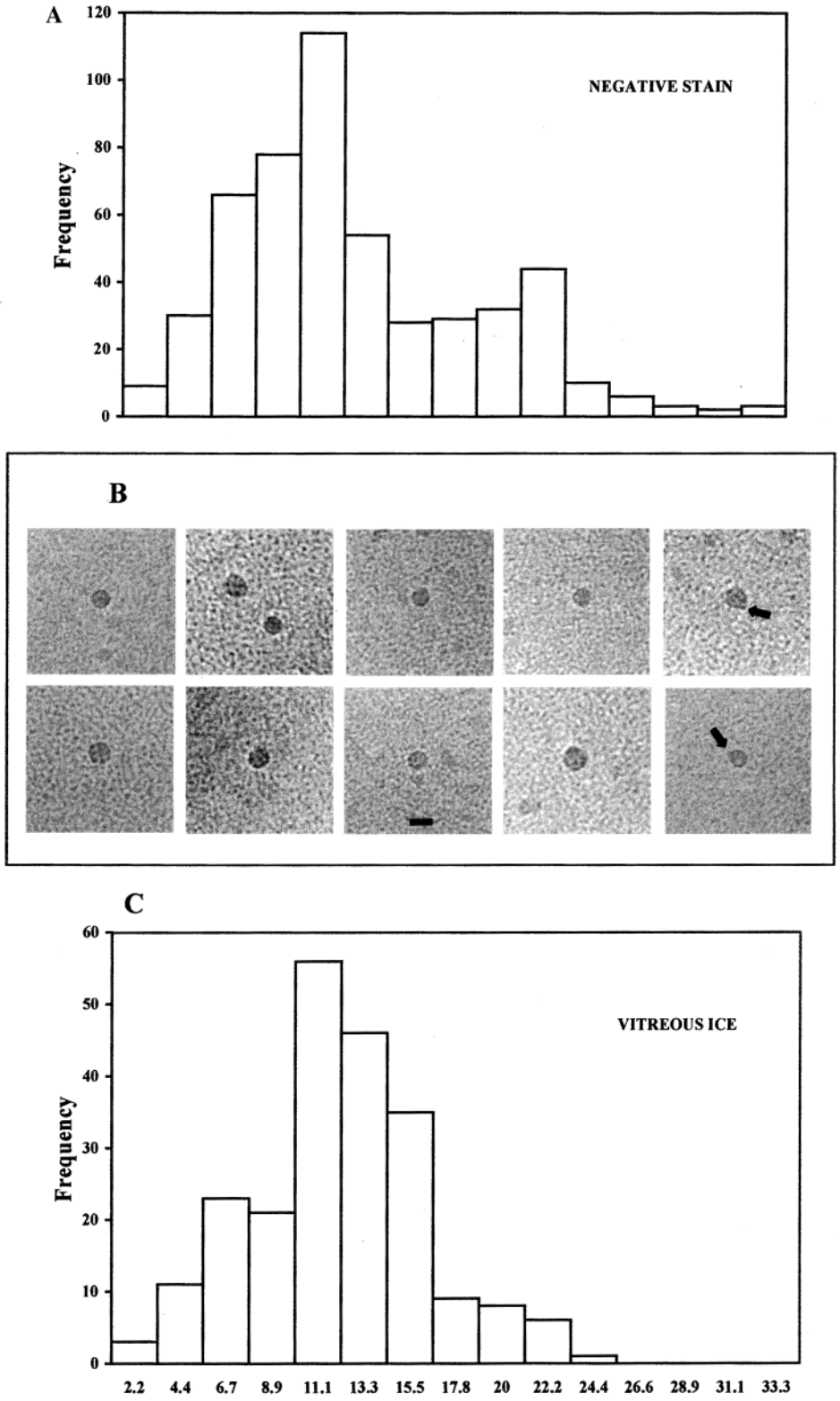

FIGURE 3: Cryoelectron micrograph and size distribution of apoB-37 particles. Cells were incubated in media supplemented with 0.8 mM oleate, collected and particles isolated as described in Figure 1. Particles were negatively stained (panel A) or trapped in vitreous ice, visualized (B), and measured as described in Materials and Methods (C). Ten examples of apoB-37 particles are shown in panel B. Bar = 15 nm. Analysis shows quasi-spherical morphology and occasional particles with a small dense projection from the surface.

acids between apoB-29 and apoB-41 we found that 368 amino acids (64%) were in predicted amphipathic β-strands of 11−15 residues. In the absence of lipid this region could displace some of the PL on the luminal surface of the ER membrane. This process could start in the translocon (*15*) or in the lumen. When diacyl glycerol acyl transferase (DGAT) is adjacent and generates TAG, this TAG binds to the hydrophobic face of the sheet (Figure 5B), forms a bulge (Figure 5C) and finally detaches (Figure 5D). Of great interest is the constant finding of some DAG in our secreted particles (Table 1). Since DAG is a molecule which converts bi-layers to inverted hexagonal structures, it is predicted to be found at concave parts of the membranes (*57*) and like other cone-shaped lipids might be implicated in the fission

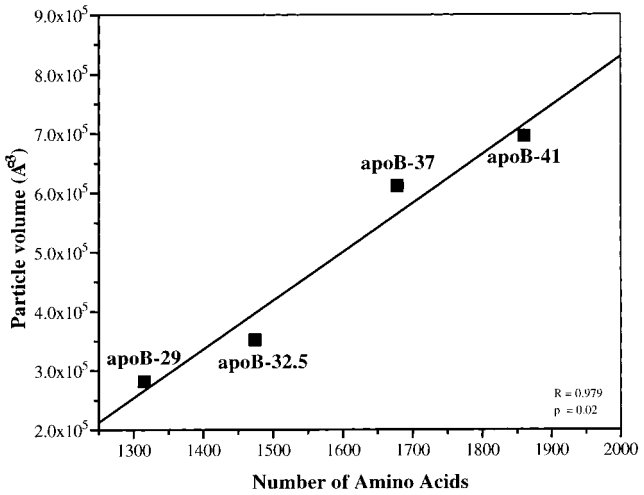

FIGURE 4: Relationship between particle volume and size of truncated apoB proteins. ApoB-containing lipoproteins recovered in density fractions from media collected after incubation of cells with 0.8 mM oleate/0.2 mM albumin were analyzed as described in Figure 1. The particle volumes were calculated based on measured particle densities and lipid composition as described in Materials and Methods.

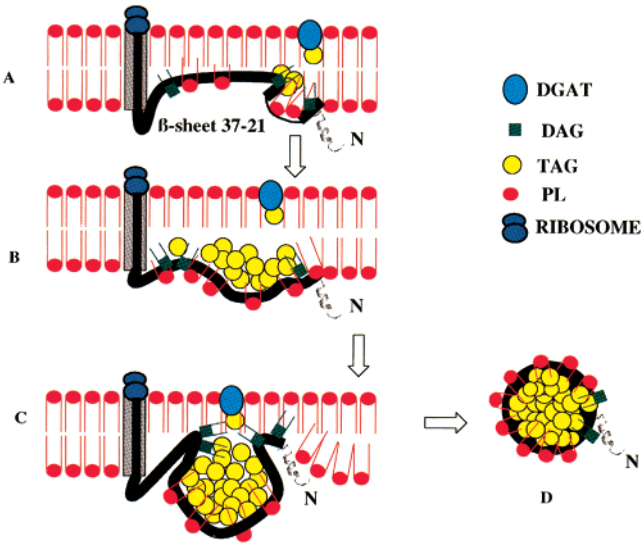

FIGURE 5: A schematic model for the cotranslational assembly of apoB-37 particles on the ER membrane in C127 cells. Following initiation of translation on ribosomes attached to the ER membrane, the N-terminal 20% of apoB interacts with the internal phospholipid leaflet of the ER and forms a "lipid-pocket" (A). The amphipathic β-sheet between apoB-21 and apoB-37 enables the pocket to fill up with TAG produced by the DGAT reaction and results in "bulging" of the particle (B and C). DAG in the concave parts of the membrane converts the bi-layer at this location into a neck structure that results in fission and release (D) of the lipoprotein from the ER membrane.

of vesicles (*58*). We suggest that in like fashion, DAG concentrate at the concave boundary of the evolving emulsion and assists in release of the lipoprotein from the ER membrane.

ACKNOWLEDGMENT

We thank Cheryl England, Michael Gigliotti, Jianying Zhang, and Gayle Forbes for their professional and enthusiastic help, Don Gantz for expert electron microscopic analysis and Dr. Aris Kritis for plasmid pUB-47.

REFERENCES

1. Brown, M. S., and Goldstein, J. L. (1986) *Science 232*, 34−47.
2. Chan, L., Chang, B. H., Nakamuta, M., Li, W. H., and Smith, L. C. (1997) *Biochim. Biophys. Acta 1345*, 11−26.
3. Schumaker, V. N., Phillips, M. L., and Chatterton, J. E. (1994) *Adv. Protein Chem. 45*, 205−48.
4. Kane, J. P., and Havel, R. J. (1995) in *The Metabolic Basis of Inherited Disease* (Scriver, Cr., B., A. L., Sly, W. S., and Valle, D., Ed.) pp 1853−85, McGraw-Hill, New York.
5. Linton, M. F., Farese, R. V., Jr., and Young, S. G. (1993) *J. Lipid Res. 34*, 521−41.
6. Schonfeld, G. (1995) *Annu. Rev. Nutr. 15*, 23−34.
7. Wu, J., Kim, J., Li, Q., Kwok, P. Y., Cole, T. G., Cefalu, B., Averna, M., and Schonfeld, G. (1999) *J. Lipid Res. 40*, 955−9.
8. Cavallo, D., McLeod, R. S., Rudy, D., Aiton, A., Yao, Z., and Adeli, K. (1998) *J. Biol. Chem. 273*, 33397−405.
9. Kim, E., Cham, C. M., Veniant, M. M., Ambroziak, P., and Young, S. G. (1998) *Clin. Invest. 101*, 1468−77.
10. Parhofer, K. G., Barrett, P. H., Aguilar-Salinas, C. A., and Schonfeld, G. (1996) *J. Lipid Res. 37*, 844−52.
11. Srivastava, R. A., Srivastava, N., Averna, M., Cefalu, A. B., and Schonfeld, G. (1999) *J. Lipid Res. 40*, 901−12.
12. Boren, J., Graham, L., Wettesten, M., Scott, J., White, A., and Olofsson, S. O. (1992) *J. Biol. Chem. 267*, 9858−67.
13. Graham, D. L., Knott, T. J., Jones, T. C., Pease, R. J., Pullinger, C. R., and Scott, J. (1991) *Biochemistry 30*, 5616−21.
14. Ingram, M. F., and Shelness, G. S. (1997) *J. Biol. Chem. 272*, 10279−86.
15. Liang, J., Wu, X., Jiang, H., Zhou, M., Yang, H., Angkeow, P., Huang, L. S., Sturley, S. L., and Ginsberg, H. (1998) *J. Biol. Chem. 273*, 35216−21.
16. Spring, D. J., Chen-Liu, L. W., Chatterton, J. E., Elovson, J., and Schumaker, V. N. (1992) *J. Biol. Chem. 267*, 14839−45.
17. McLeod, R. S., Wang, Y., Wang, S., Rusinol, A., Links, P., and Yao, Z. (1996) *J. Biol. Chem. 271*, 18445−55.
18. Wang, H., Yao, Z., and Fisher, E. A. (1994) *J. Biol. Chem. 269*, 18514−20.
19. Wu, M. J., Chen-Liu, L. W., Xiao, Q., Phillips, M. L., Elovson, J., Linton, M. F., Young, S. G., and Schumaker, V. N. (1997) *J. Lipid Res. 38*, 2473−82.
20. Yao, Z. M., Blackhart, B. D., Linton, M. F., Taylor, S. M., Young, S. G., and McCarthy, B. J. (1991) *J. Biol. Chem. 266*, 3300−8.
21. Young, S. G., Krul, E. S., McCormick, S., Farese, R. V., Jr., and Linton, M. F. (1996) *Methods Enzymol. 263*, 120−45.
22. Herscovitz, H., Hadzopoulou-Cladaras, M., Walsh, M. T., Cladaras, C., Zannis, V. I., and Small, D. M. (1991) *Proc. Natl. Acad. Sci. U.S.A. 88*, 7313−7.
23. Herscovitz, H., Kritis, A., Talianidis, I., Zanni, E., Zannis, V., and Small, D. M. (1995) *Proc. Natl. Acad. Sci. U.S.A. 92*, 659−63.
24. Laemmli, U. K. (1970) *Nature 227*, 680−5.
25. Dubochet, J., Adrian, M., Chang, J. J., Homo, J. C., Lepault, J., McDowall, A. W., and Schultz, P. (1988) *Q. Rev. Biophys. 21*, 129−228.
26. Gantz, D. L., Wang, D. Q., Carey, M. C., and Small, D. M. (1999) *Biophys. J. 76*, 1436−51.
27. Spin, J. M. (1997) in *Ph.D. Thesis, Biophysics Department*, Boston University School of Medicine, Boston.
28. Mann, C. J., Anderson, T. A., Read, J., Chester, S. A., Harrison, G. B., Kochl, S., Ritchie, P. J., Bradbury, P., Hussain, F. S., Amey, J., Vanloo, B., Rosseneu, M., Infante, R., Hancock, J. M., Levitt, D. G., Banaszak, L. J., Scott, J., and Shoulders, C. C. (1999) *J. Mol. Biol. 285*, 391−408.
29. Anderson, T. A., Levitt, D. G., and Banaszak, L. J. (1998) *Structure 6*, 895−909.
30. Young, S. G., Bertics, S. J., Curtiss, L. K., and Witztum, J. L. (1987) *J. Clin. Invest. 79*, 1831−41.
31. Young, S. G., Pullinger, C. R., Zysow, B. R., Hofmann-Radvani, H., Linton, M. F., Farese, R. V., Jr., Terdiman, J. F., Snyder, S. M., Grundy, S. M., and Vega, G. L. (1993) *J. Lipid Res. 34*, 501−7.

32. Boren, J., Rustaeus, S., and Olofsson, S. O. (1994) *J. Biol. Chem*. *269*, 25879−88.
33. Adeli, K., Macri, J., Mohammadi, A., Kito, M., Urade, R., and Cavallo, D. (1997) *J. Biol. Chem*. *272*, 22489−94.
34. Chen, Y., Le Caherec, F., and Chuck, S. L. (1998) *J. Biol. Chem*. *273*, 11887−94.
35. Liao, W., Yeung, S. C., and Chan, L. (1998) *J. Biol. Chem*. *273*, 27225−30.
36. Linnik, K. M., and Herscovitz, H. (1998) *J. Biol. Chem*. *273*, 21368−73.
37. Ou, W. J., Cameron, P. H., Thomas, D. Y., and Bergeron, J. J. (1993) *Nature 364*, 771−6.
38. Patel, S. B., and Grundy, S. M. (1996) *J. Biol. Chem*. *271*, 18686−94.
39. Tatu, U., and Helenius, A. (1999) *Biosci. Rep. 19*, 189−96.
40. Dixon, J. L., Furukawa, S., and Ginsberg, H. N. (1991) *J. Biol. Chem*. *266*, 5080−6.
41. McCormick, S. P., Day, W. A., and George, P. M. (1995) *Biochim. Biophys. Acta 1258*, 49−56.
42. Nolte, R. T. (1994) in *Ph.D. Thesis*, *Biophysics Department*, Boston University School of Medicine, Boston.
43. Segrest, J. P., Jones, M. K., Mishra, V. K., Anantharamaiah, G. M., and Garber, D. W. (1994) *Arterioscler. Thromb. 14*, 1674−85.
44. Small, D. M., and Atkinson, D. (1997) *Circulation 96*, 1.
45. Burch, W. L., and Herscovitz, H. (2000) *J. Biol. Chem*. *275*, 16267−16274.
46. Gretch, D. G., Sturley, S. L., Wang, L., Lipton, B. A., Dunning, A., Grunwald, K. A., Wetterau, J. R., Yao, Z., Talmud, P., and Attie, A. D. (1996) *J. Biol. Chem. 271*, 8682−91.
47. Hussain, M. M., Bakillah, A., Nayak, N., and Shelness, G. S. (1998) *J. Biol. Chem. 273*, 25612−5.
48. Shelness, G. S., and Thornburg, J. T. (1996) *J. Lipid Res. 37*, 408−19.
49. Tran, K., Boren, J., Macri, J., Wang, Y., McLeod, R., Avramoglu, R. K., Adeli, K., and Yao, Z. (1998) *J. Biol. Chem*. *273*, 7244−51.
50. Segrest, J. P., Jones, M. K., and Dashti, N. (1999) *J. Lipid Res. 40*, 1401−16.
51. Hamilton, R. L., Erickson, S. K., and Havel, R. J. (1995) *Nascent VLDL assembly occurs in two steps in the endoplasmic reticulum (ER) of hepatocytes*, Elsevier Science, Amsterdam.
52. Hamilton, R. L., Wong, J. S., Cham, C. M., Nielsen, L. B., and Young, S. G. (1998) *J. Lipid Res. 39*, 1543−57.
53. Murphy, D. J., and Vance, J. (1999) *Trends Biochem. Sci. 279*, 109−115.
54. Olofsson, S. O., Asp, L., and Boren, J. (1999) *Curr. Opin. Lipidol. 10*, 341−6.
55. Nolte, R. T., and Atkinson, D. (1992) *Biophys. J. 63*, 1221−39.
56. White, J. V., Stultz, C. M., and Smith, T. F. (1994) *Math. Biosci. 119*, 35−75.
57. Hindenis, J. O., Nerdal, W., Guo, W., Di, L., Small, D. M., and Holmsen, H. (2000) *J. Biol. Chem. 275*, 6857−67.
58. Schmidt, A., Wolde, M., Thiele, C., Fest, W., Kratzin, H., Podtelejnikov, A. V., Witke, W., Huttner, W. B., and Soling, H. D. (1999) *Nature 401*, 133−41.

BI000791H